Biomimetic Intestine for Traction Force Studies

BME Design 300/200
December 11th, 2013

TEAM MEMBERS:
Angela Beltrame-BPAG
Kevin Knapp-BSAC
Susanna Kwok-Communicator
Shaun Pomerenke-BWIG
Conor Sullivan-Team Leader

CLIENT:
Professor Michael Murrell
Department of Biomedical Engineering
University of Wisconsin-Madison

ADVISOR:
Professor Randolph Ashton
Department of Biomedical Engineering
University of Wisconsin-Madison

Abstract

Epithelial cell migration and turnover on the villus structure of the human small intestine is a relatively unexplained phenomenon. It has been hypothesized that epithelial cells migrate from crypt to villus due to various biochemical factors and traction forces produced by the topography of the small intestine and the various forces imposed by fluid flow. In order to quantify and study these traction forces, it is critical to construct an accurate model of intestinal villi, featuring accurate topography and size scaling. A three-dimensional collagen scaffold featuring rounded, micro-needle arrayed topography is desired for such a model. Following seeding of epithelial cells on this scaffold, we hope to create a biomimetic model of the intestine. To generate uniform scaffolds, we investigated methods of creating a plastic, master mold used for the generation of a 3D collagen scaffold. Methods were judged based on their ability to generate accurate villi structures of varying diameter (100-500μm), variations of villus height (500-1000μm), and rounded tips. We found three methods that fit these criteria: UV-LIGA, multi-photon excited photochemistry, and UV/CO_2 laser ablation. These three methods were evaluated based on ease of fabricating the master mold, access to equipment, reproducibility of the methods, amount of training required, cost, and other factors. The laser ablation method, featuring the use of either a UV or CO_2 laser was determined to be the most effective at generating a master mold with our desired features. However, due to limitations of the CO_2 laser diameter and the inability of the laser to generate curved micro-needle arrays of controlled height, our group decided to use the second method designated by our design matrix, multi-photon excitation photochemistry. Using this method, our group was able to generate prototype villus structures featuring tapered pillars with curved tips with accurate diameter and height dimensions.

Table of Contents

Background

Physiology of Intestinal Villi

The epithelial lining of the mammalian small intestine is structured into millions of tiny, finger-like projections called villi (Sherwood, 2011). Villi are comprised of a lacteal vessel, blood vessels, muscular tissue, and a mucosa layer all covered by a single cell layer of absorptive cells known as enterocytes (Sherwood, 2011). Nearly all nutrients, including amino acids and sugars, enter the systemic blood pathway by crossing the epithelium covered villi (Bowen, 2001). Following entry through the epithelial layer, nutrients are either diffused into the capillary network or carried by the lymphatic vessel (lacteal) located within each villus (Bowen, 2001). The purpose of the villus structure is to increase absorptive surface area in the small intestine (Sherwood, 2011). Villi typically project 1mm into the intestinal lumen and feature a variety of cross-sectional diameters with an average diameter of 0.5mm in the human small intestine (Sherwood, 2011; Caceci, 2013). Each villus is separated by deep invaginations known as Crypts of Lieberkuhn (Sherwood, 2011). In the crypts, enterocytes begin their life cycle as proliferating stem cells that propagate the constant regeneration of the epithelial cell layer (Brunicardi et al., 2005).

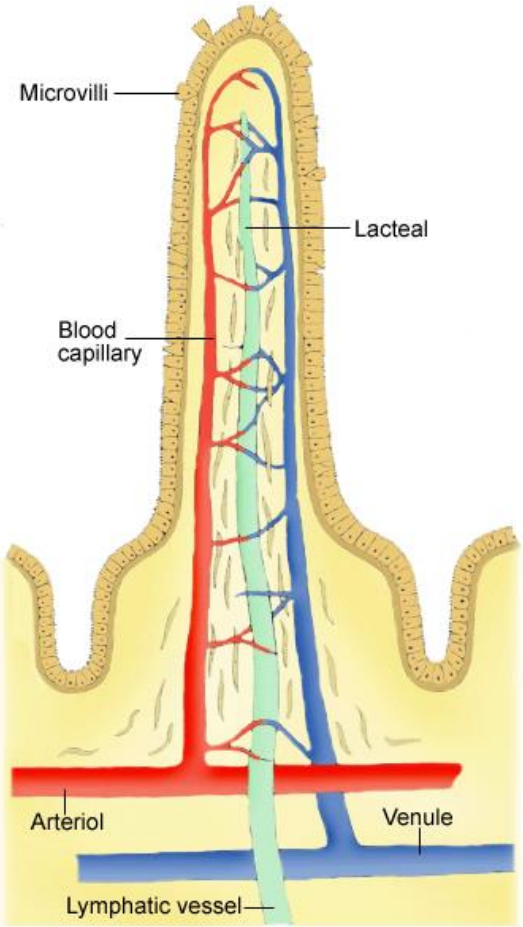

Figure 1: Components of the intestinal villi depicting enterocytes on epithelial layer. (Proffitt et al., 2013)

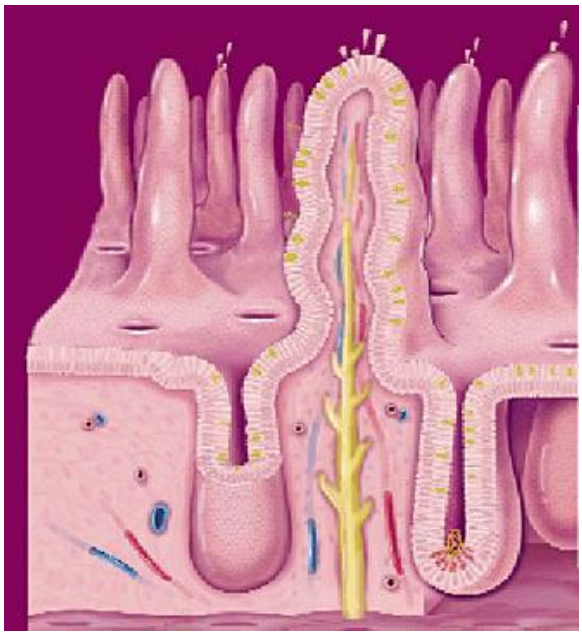

Figure 2: Relationship between crypt and villi (Ganz et al., 2000)

With each stem cell division, one daughter cell remains in the crypt while the other differentiates into one of four cell types, with the principal lineage being the enterocyte (Bowen, 2001). As enterocytes age, they divide and migrate up the sides of the villus (Bowen, 2001). At maturity, enterocytes are exceptional absorption cells, expressing numerous transport proteins and enzymatic characteristics, which are key to their function (Bowen, 2001). At the tip of the villus, they perish and shed off into the lumen for reabsorption (Brunicardi et al., 2005). The small intestine lining undergoes continuous renewal due to the coordinated movement of enterocytes from crypt to villus tip during their life cycle of 24 - 48 hours (Brunicardi et al., 2005). The mechanisms underlying the rapid turnover of enterocytes in the small intestine are relatively unknown; however, it is hypothesized to be highly reliant on cell adhesion and traction forces (Basson, 2008).

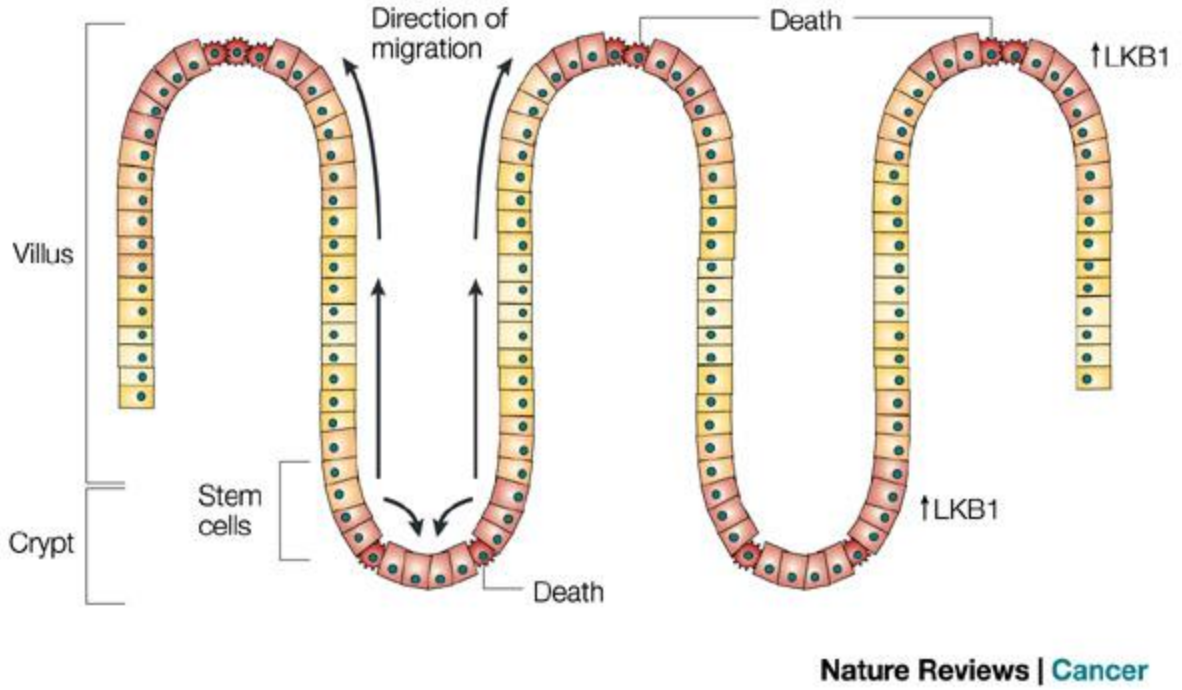

Figure 3: Migration of enterocytes from crypt to villus and subsequent cell life-cycle stages (Yoo et al., 2002)

Client Information

Professor Michael Murrell, a faculty member of the Department of Biomedical Engineering at the University of Wisconsin-Madison, is interested in studying the factors and mechanisms underlying enterocyte migration in the small intestine. He is particularly interested in the traction forces caused by villi structure and their effects in the coordinated movement of enterocytes. In order to directly measure the traction forces involved in enterocyte migration, he would like to fabricate a realistic model of an intestine featuring three-dimensional (3D) villus topography and proliferating epithelial cells to be seeded on the villus structures. To better understand the effects of villus structure on enterocyte migration, he would like a model in which villus diameter and height could be varied. Additionally, he would like an easily replicable method of generating this biomimetic intestine.

Client's Requirements & Design Constraints

The client has given several requirements regarding the specification of the final villi scaffold. First and foremost, the scaffold must be a micro-needle array with specified topography. This topography must be a tapered, conical tip on each cylindrical "villus" pillar. Another topographical constraint given to us is a minimum of 250µm spacing between the base perimeters of neighboring villus pillars. The spacing pattern will be maintained across the entire microarray scaffold to provide a uniform crypt bed between the villi projections, regardless of pillar diameter. In order for Professor Murrell to study the effects villi size plays on cell forces, we must create an array of pillar diameters with set increments. The diameters to be fabricated on the mold are 100 µm, 200 µm, 300 µm, 400 µm and 500 µm. The heights of the villi are to be

varied from a range of 500 μm to 1000 μm. Each of these five sizes in conjunction to the variations in height must be present in the final mold. Secondly, the final scaffold must be produced out of methacrylated collagen type I. Additionally, our client's budget for the fabrication of the master mold and production of the collagen scaffold is $1000 USD.

Problem Statement

Mechanisms which underlie the coordinated migration of enterocytes from crypt to villus are unknown and have yet to be studied in an *in vitro* system. In order to observe and measure the cellular adhesion forces and traction forces involved in the rapid turnover of enterocytes within the small intestine, a precise model of the intestinal villi is needed. This model must feature realistic 3D topography of the small intestine, defined by round-tipped, conical structures to imitate villi. Ideally, this model would be fabricated using biologically compatible hydrogel scaffolding such as collagen; 3D structures on collagen scaffold would be seeded with intestinal epithelial cells in order to create a biomimetic model of the human small intestine. The creation of this biomimetic model would allow for the observation, direct measurement, and manipulation of variables involved in enterocyte migration.

Methods

A variety of methods exist for the creation of 3D topography on collagen scaffold, however, methods yielding highly reproducible, uniform scaffolds generally involve the fabrication of a master mold. This mold would then be used to create subsequent collagen molds featuring a positive volume that matches the desired 3D shape of the scaffold. For our purposes, and per client specifications, the creation of a master mold followed by collagen addition and polymerization from the mold will be the general methods used for the creation of collagen scaffold. Although we have defined a general method for the creation of 3D structures on collagen, methods for the creation of the master mold used in this process are still undefined.

Current Methods

Methods used for the generation of a plastic master mold used for soft lithography are constrictive. Most methods can only fabricate square pillar topography. These structures do not accurately represent the 3D rounded-tip, conical structure of villi. There are currently several methods of creating structures similar to the villi of the small intestine on a micron-scale sizing. Current methods include photolithography and micro-contact printing. Photolithography is a process where a material is exposed to light radiation, usually UV radiation, and will polymerize where the material comes into contact with light (Phillips, 1984). Then, the parts that were not irradiated are dissolved and eroded away, leaving the desired structures with a flat top (Phillips, 1984). Another process, micro-contact printing, builds a blueprint of a schematic block by block in a layer fashion (Jee et al., 2000). Structures generated using this method, however, are fairly blocky due to the fact that each part of a model in 3D printing is put down as a sphere and leaves small indentations between the intersections of each sphere (Sachs et al, 1997).

Methods for Biomimetic Scaffold Generation

In order to create a biomimetic model of the small intestinal villi, our plan is to generate a three-dimensional methacrylated type-I collagen scaffold through the use of a plastic, TMPTA master-mold (Figure 4). After obtaining a negative master-mold, liquid methacrylated type-I collagen containing fluorescent microsphere beads will be injected into the negative mold and polymerized under 365nm of light (Figure 4) (Gaudet et al., 2012). Following the polymerization of liquid type-I collagen to solid form, the scaffold would be removed. Epithelial stem cells will then be seeded on top of the scaffold, covering all the villus structures. Stem cell seeding will take place over a period of 21 days in order to coat the entire villi surface (Yu et al., 2012). Following stem cell seeding, traction forces studies will be performed.

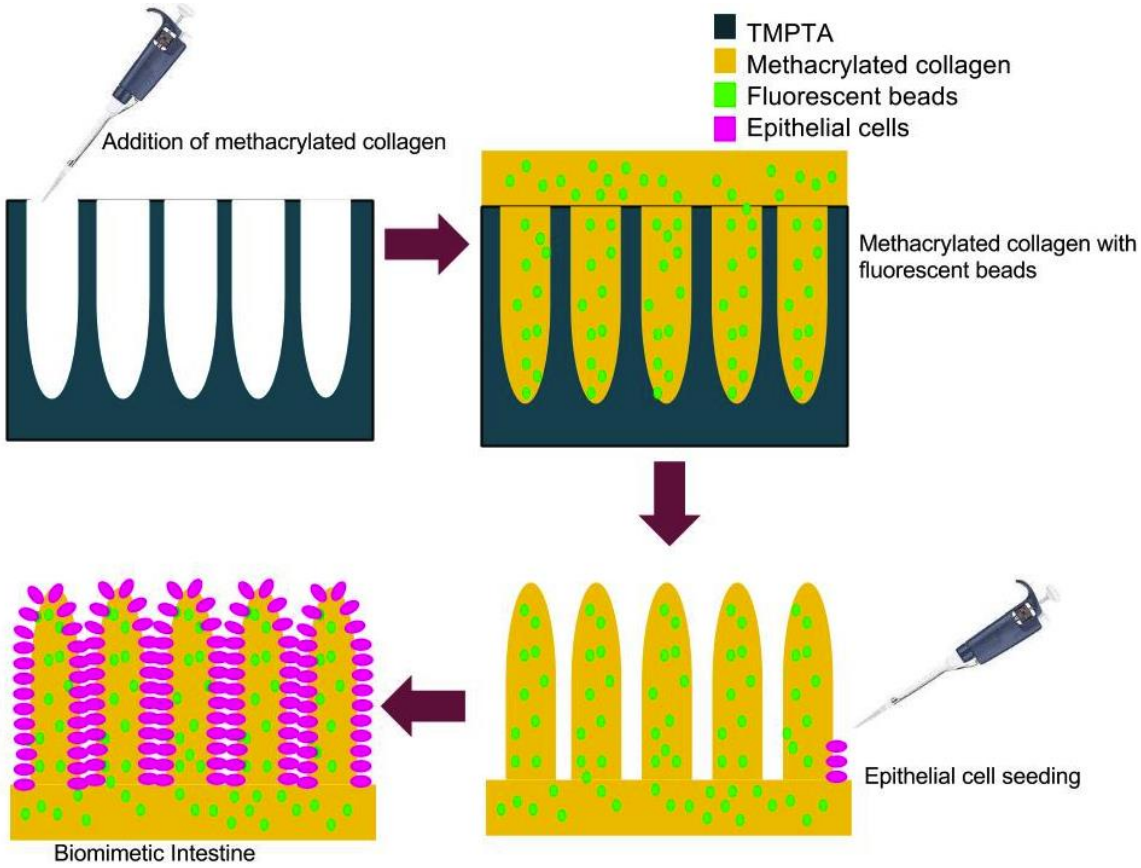

Figure 4: Schematic detailing the fabrication of a biomimetic villi scaffold using a TMPTA master-mold (Image generated using GoogleDraw)

Type-I Collagen

Type-I Collagen is the most abundant collagen protein found in the human body; it is a major component of bone, tendon, skin, ligament, and other interstitial connective tissues (Gelse et al., 2003). Collagen is made up of microfibrils that have an average diameter of 50nm and are composed of protein α-chains of repeating amino acids, glycine, proline, and hydroxyporline (Lodish et al., 2000). These α-chains are arranged in a triple helix to create collagen microfibrils

(Lodish et al., 2000; Gelse et al., 2003). Microfibrils collectively form collagen fibrils that then make up collagen fibers (Figure 5) (Lodish et al., 2000; Gelse et al., 2003). Due to its abundance and biocompatibility, collagen type-I is commonly used for tissue engineering purposes (Chevallay et al., 2000; Gaudet et al., 2012). For use in 3D scaffolding processes, however, collagen type-I has inherent flaws, namely the lack of inherent rigidity that make it unsuitable to maintain 3D structures under cell load (Glowacki et al., 2007). Additionally, mechanical properties cannot be modified or controlled using collagen type-I (Gaudet et al., 2012).

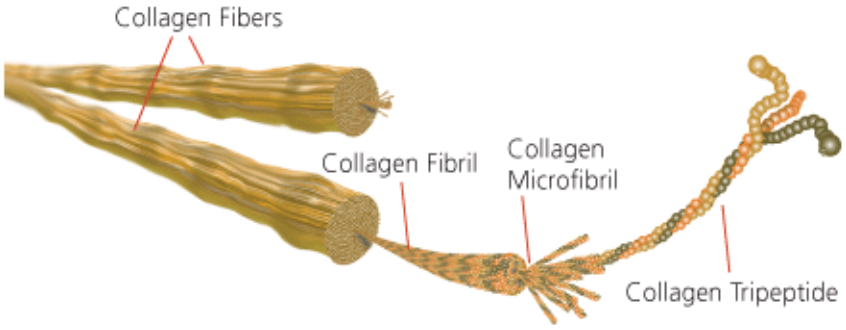

Figure 5: Structural components of collagen fibers (Sigma Aldrich, 2013)

Methacrylated Type-I Collagen

Although collagen type-I is unsuitable for use in 3D scaffolds, modified collagen can provide greater rigidity and control over stiffness (Gaudet et al., 2012). Modifications to type-I collagen can be made by chemically cross-linking methacrylate groups to the triple helix structure of collagen (Gaudet et al., 2012). Methacrylated type-I collagen is an attractive alternative to type-I collagen because it is easy to modulate its mechanical properties through photocrosslinking the light-sensitive methacrylate groups (Gaudet et al., 2012). Additionally, methacrylated type-I collagen retains the fundamental features of collagen such as biocompatibility, biodegradability, and cellular adhesivity (Gaudet et al., 2012). In addition to improving control over mechanical properties, methacrylated type-I collagen is known to degrade at a slower rate compared to type-I collagen which makes it an ideal hydrogel for culturing cells over a long period of time (Gaudet et al., 2012).

Scaffold Complications

In order to provide an optimal environment for cell proliferation and growth, an ideal collagen scaffold should be highly porous and permeable (Yao et al., 2005). These characteristics, however, cause structural instability in 3D microstructures fabricated from type-I collagen; therefore, 3D topographic generated on scaffold typically break upon release from a master mold (Golden et al., 2006). Although our methods involve the use of stiffer and more rigid methacrylated type-I collagen, we may still face issues regarding improper scaffold release from the master mold; namely, shear forces generated between the master mold and the solid collagen may break off the tips of the villus structures. In order to counter this effect, additional

steps may be added to our scaffold generation methods. Sacrificial molding, a technique often used to prevent fracturing of the 3D structures generated on collagen, could be used in conjunction with the existing methods for collagen scaffold generation (Figure 4) (Golden et al., 2006; Sung et al., 2011; Yu et al., 2012). Sacrificial molding often involves the use of a dissolvable sacrifice mold in order to avoid inducing shearing forces between a master mold and the generated scaffold (Golden et al., 2006; Sung et al., 2011; Yu et al., 2012). To use sacrificial molding, our methods would adopt additional molding processes in which a positive mold, made of another polymer, would be made using the master mold (Figure 6). Additionally, a hydrogel/polymer that can be dissolved using a solution that does not degrade collagen would be used to create a negative reverse mold using this newly generated positive mold (Figure 6). Finally, this dissolvable hydrogel/polymer would be used to generate the desired collagen mold (Figure 6). However, following the polymerization of the collagen, the mold around the scaffold will be dissolved. This would release the collagen scaffold without inducing shear forces (Golden et al., 2006; Sung et al., 2011; Yu et al., 2012).

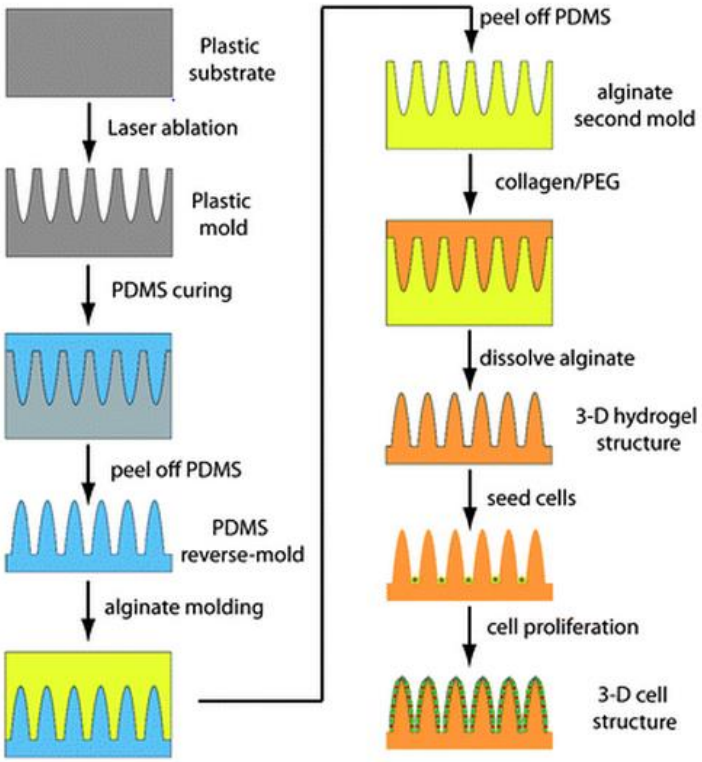

Figure 6: Overall fabrication process (Sung et al., 2011)

Method Alternatives

Multi-photon Excited (MPE) Photochemistry

One possible method to make the master mold is through the use of multiphoton excited (MPE) photochemistry. This method is currently being utilized at UW-Madison in Professor Campagnola's Lab. A grad student there, Visar Ajeti, is very enthusiastic about our

project and offered to build the mold for us using this method. MPE photochemistry uses a laser to build 3D structures out of a variety of compounds, such as plastic or proteins (LaFratta, 2007).This is done by using computer aided software to control galvanometer mirrors which aim two or more photon beams onto the photopolymerizable material (Cunningham et al, 2006). These focused photon beams cause the molecules of the photopolymerizable material to become excited. This excitation causes the material to form cross-links in the 2D plan; 3D shapes can be formed by lowering the stage in the z direction (Chen et al, 2012). This method is incredibly precise since it can target one individual monomer without polymerizing neighboring monomers (Multiphoton polymerization, 2013).

This method is able to produce objects with heights of 1-1000μm and diameters of 1-800μm (LaFratta, 2007). These dimensions fall within the specifications of our project. The negative mold constructed from this project could be formed with TMTPA, a polymerizable polymer which forms into a hard plastic.

UV/CO2 Laser Ablation

The use of laser ablation for microfabrication has been steadily gaining momentum in the creation of three dimensional, microstructures (Waddell, 2006). Laser ablation systems can differ depending on the type of light used; UV laser ablation systems feature the use of ultraviolet radiation having wavelength of roughly 355nm whereas CO2 laser systems feature the use of infrared radiation having a wavelength range of 9.3μm to 10.6μm (Lange, B., 2013). Both systems function in a similar manner, namely both utilize highly concentrated, powerful beams of radiation to break chemical bonds in metals and polymers in order to 'etch' materials (Lange, B., 2013; Waddell, 2006). Laser ablation systems feature the ability to freely manipulate in the x, y, and z direction by controlling laser intensity, length of exposure, and repeat exposure of material to the laser (Lange, B., 2013). Furthermore, most laser ablation systems are computer controlled, meaning program files featuring 2D or 3D design (such as CAD files or Corel Draw files) can be inputted into software that feeds into control of the laser (Yu et al., 2012).
Both systems offer precise resolution; CO2 laser ablation systems can etch diameters as small as 75μm (Lange, B., 2013). UV laser ablation systems are more precise and refined than CO2 laser ablation systems; they can etch diameters as small as 30μm featuring a high aspect ratio (Lange, B., 2013). The lack of materials required for fabrication, precision, and automation featured by laser ablation makes it an attractive method for the fabrication of 3D, microscale structures.

UV-LIGA

UV-LIGA stands for the German words meaning lithography, electroplating, and molding (Yang et al., 2012). This method features the creation of a photo-resistive mask, typically made from a chromium plate; etched using computer aided engraving (Ghodssi et al., 2011). For our purposes, this mask will resemble a plate with numerous circles of various diameters as negative area. SU-8 an epoxy based, negative photoresist will be used as the polymer for the master mold generating using this method (Lorenze et al., 1997). SU-8 starts out as a gel-like polymer, but it polymerizes into a hard polymer when exposed to heat or UV-light

(Lorenz et al., 1997; Yang et al., 2012). In order to use SU-8 as our substrate, gel-like SU-8 will be put onto a glass plate coated with titanium and spun at 500 revolutions per minute for thirty seconds (Yang et al., 2012). Following spinning, the SU-8 will be baked at 90 degrees Celsius for three hours (Yang et al., 2012). The SU-8 is then removed from the glass and layered with a photo-resistive resin followed by the chromium mask. SU-8 is a compound that polymerizes through cross-linking as it is exposed to UV-light (Lorenze et al., 1997). Therefore, as UV-light contacts the area not covered by the photo-resistive mask, it will polymerize and form 3D structures. The methods used to generate microneedle arrays using UV-LIGA feature a backside exposure of the SU-8 to UV light (Yang et al., 2012). The height of the arrays depends solely on the length of exposure the SU-8 has to UV light, but typically has a maximum resist height of around 800um-1000um and a minimum lateral size of 0.2um (Ghodssi et al., 2011). Following these steps, a master mold of SU-8 would be created; however, prior to usage as a mold, SU-8 must be layered with a mixture of titanium and gold (Yang et al., 2012). A 30nm/100nm layer of Ti/Au can be added onto the SU-8 via sputtering (Yang et al., 2012). This metallic layer prevents subsequent molds made by PDMS, created using the SU-8 mold, from adhering to the SU-8 (Yang et al., 2012). The main attractive feature of this method is the ease of equipment use and access; without considering the engraving of the chromium mask, UV-LIGA requires only the use of a UV-light source (a mercury lamp), a spinerette, and a hot-plate or oven.

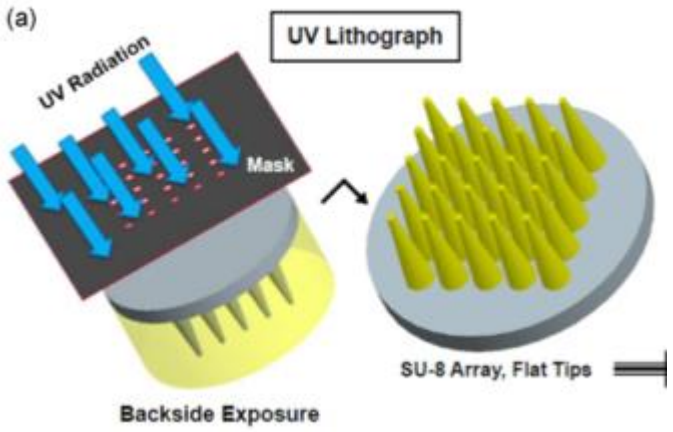

Figure 7: Backside exposure of UV radiation to SU-8 substrate to form microneedle array (Yang et al., 2012)

DESIGN MATRIX

After selecting our three method alternatives for the fabrication of the master mold, the methods were compared and contrasted using scaled criteria featured in a design matrix. Our design matrix is unconventional because methods, not products, are being compared.
The design of our product will be the same for each proposed method. We will be comparing three methods: MPE photochemistry, CO2 laser ablation, and UV-LIGA. Based off of client specifications and features we deemed important, the eight criteria in our design matrix were chosen. The criteria are listed in the order of their importance to the methodology: ease of fabrication, access to equipment, reproducibility, training, time, cost, durability, and safety.

Design Criteria (Weight)	Laser Ablation		MPE Photochemistry		UV-LIGA	
Ease of Fabrication (25)	4	20	3	15	2	10
Access to Equipment (15)	3	9	5	15	1	3
Reproduceability (15)	5	15	1	3	4	12
Training (15)	4	12	5	15	2	6
Time (10)	5	10	3	6	2	4
Cost (10)	5	10	3	6	2	4
Durability (5)	3	3	3	3	3	3
Safety (5)	3	3	4	4	3	3
Total (100)		**82**		**67**		**45**

Figure 8: Design Matrix

Ease of Fabrication

Ease of fabrication is our most important criteria, and therefore we gave it a weight of twenty five points. This is the most important factor in our design problem because of the incredibly small scale of our final design. With villi ranging from five to five hundred micrometers, our final product will be no longer than seven centimeters in total. Therefore, we need a method that makes creating this mold as precisely and easily as possible. Laser ablation won this category with a score of a four out of a five because it is almost entirely computer automated and very accurate. Unlike the other two designs, which must be made in labs and possibly result in error, laser ablation takes a computer aided design file and can accurately create it without introducing human error.

Access to Equipment

The next three categories are all equally weighted; however, access to equipment is slightly more important and was placed next in the list. Access to equipment is important to our project due to the size of our master mold. Going hand-in-hand with ease of fabrication, having easy access to equipment is important as there are not many methods capable of producing molds in microscale. MPE Photochemistry won this category with a score of five out of five because the equipment necessary for performing this method is located in the Engineering Centers Building, housed in Professor Campagnola's lab. Laser ablation received a score of three. Despite hearing numerous mentions of this laser ablation system, it remains elusive.

Reproducibility

Another important criterion is reproducibility which was also assigned fifteen points. Reproducibility would give Professor Murrell the ability to use our methods and make his own alterations. This criterion is important to Professor Murrell, because future studies may include

the addition of different diameter cross sections, heights, or a combination of both features. Therefore, methods for generating the master mold must be easy to reproduce. Laser ablation received five out of five points for this category because it can be drawn up in a CAD file and created by a laser, resulting in minimal work for our client.

Training

The last criterion, worth fifteen points is the amount training required before fabrication can begin. Many of the methods we researched required the use of very expensive machinery and extensive training. Methods involving extensive training were weighted quite heavily in our design matrix. Professor Murrell believed that intense training hinders the time of fabrication and negatively affects reproducibility. This is true for MPE photochemistry; however, Professor Campagnola's lab is willing to create our mold for us. Therefore, we would require no training; as a result, this method received a score of a five out of five.

Time

Time is also an important factor and received a weight of ten points. We want a method that is accurate and quick to produce a master mold. Since we only have one semester to fabricate a biomimetic intestine, the method we choose cannot take months to create. Laser ablation won this category with a score of five out of five because it is a process that can be done in less than a week. Unlike MPE Photochemistry and UV-LIGA which involve chemicals and coatings of metals, laser ablation simply cuts into plastics. Clearly this process is much simpler and quicker, resulting in an obvious win in this category.

Cost

Along with time, cost is also an important criterion to our client. Professor Murrell supplied us with a budget of $1000; however, we would like to minimize our costs as much as possible. It was challenging to compare the costs of all three methods; however, we did our best to estimate. We were able to determine cost of all materials necessary for laser ablation; it came to a total of $350.40 without accounting for a possible laser operating fee. Operating fees may apply to the other methods as well. Unlike MPE photochemistry and UV-LIGA, CO2/UV laser ablation requires only one material, PMMA. MPE photochemistry and UV-LIGA both requires the purchase of SU-8, photo-resistive resin, Ti/Au layering substrate, and other additional chemicals. Furthermore, MPE photochemistry would require us to pay an outsourcing fee to Professor Campagnola's lab. In conclusion, laser ablation won this category with a score of five out of five based on our projections for the costs of all of the methods.

Durability

Durability and safety tied for the lowest weighted criteria, both having five points each. Durability is a criterion that Professor Murrell wanted us to include in our design matrix. He wants a mold that can withstand multiple usage. However, as a group, we determined that the

mold created by any of these methods would all be made of equally durable material. Therefore, there was a tie between all of our designs in this category with a score of three out of five.

Safety

Our last criterion is safety with a weight of five points. All of our methods are fairly safe to use, and therefore safety was not rated highly. Our scores for this criterion were very similar, however, MPE photochemistry won this category with a score of four out of five because we would be outsourcing it to Professor Campagnola's lab and would not need to interact with the equipment nor the chemicals involved in the process.

Total Scores

Following score addition, we determine that laser ablation was the best method, having a score of 82. MPE Photochemistry placed second with a score of 67. Finally UV-LIGA placed last with a score of 45. All of these scores are out of a possible 100 points. The large discrepancies between the methods in our matrix clearly show laser ablation is the best method. However, no matter which method we choose, all of them have inherent challenges that we will have to face when moving forward with our project.

Complications

There were multiple complications throughout the course of the semester that altered our course of action and decision making. At the time of the mid semester report, we had decided to use the UV-laser ablation system to create our mold based on our design matrix results. We managed to locate two carbon dioxide lasers on campus: one in the Wisconsin Institute for Discovery and one in the College of Engineering Student Shop. While the laser located in the Wisconsin Instituted for Discovery had a power of 60 watts, it was also much more difficult to gain access to. The laser located in the College of Engineering Student Shop had a power of 40 watts and was easily available.

We met with Charles "Chuck" Allhands who is an instrument maker in the instrument show. Since this laser was only recently added to the Student Shop from the Biomedical Resource Room, Chuck was not aware of its full capabilities. He trained us on how to use it and offered us the opportunity to experiment with the various machine settings to see if it would reach our client specifications and could therefore be used for our project.

We spent two weeks being trained, reading the Epilog manual, brainstorming tests, and experimenting with the machine until we realized the laser engraver did not have the capabilities we were looking for. We tested the diameter of the laser and determined it to be 432 microns; this diameter is too large to cut the 100, 200, 300 and 400 micron diameters of the client specifications. Another complication with this laser is that it would need a very high resolution picture to be printed by the machine. Also, the machine did not have the capabilities to create structures on the 100 micron scale without making them uneven. Even with a broad range of settings, the Epilog machine could not accurately produce parabolic structures.

Design Matrix Revisited

As a result of these difficulties, we returned to our design matrix to explore our options. MPE photochemistry was our second best method, with a score of 67. The benefits of the MPE

photochemistry method includes access to the equipment, training required, and safety: MPE photochemistry scored the highest in these categories. Access to equipment scored high because it is located on the second floor of the Engineering Centers Building in the Campagnola Lab. This method scored highest for training since no training was required because we outsourced all of the work to the Campagnola Lab. Finally, it also scored highest for safety because there would be no health risks for us since we outsourced the work.

After deciding to pursue the MPE photochemistry method, we met with Visar Ajeti, who offered to help us. We explained our project to him and he seemed fairly certain he could meet almost all of the client specifications using the equipment he had. He would be able to created diameters ranging from 1µm to 800µm, which greatly exceeds our client specifications. He would also be able to create a mold that had the correct spacing of 250µm between each base. One client specification he would not be able to satisfy would be the height of 1000µm. The microscope Visar uses in the process of MPE photochemistry has a maximum height of 1000µm from the stage to the objective lens. To prevent the object from adhering to the microscope lens, Visar was willing to produce an object with a maximum height of 950µm, including 50µm under each well so that he mold could adhere to the slide. This would allow for maximum heights of 900µm. After using our design matrix and learning this from Visar, we decided to pursue this method of fabrication for the remainder of the semester.

The only issue is with the final fabrication. The time it takes to make just one villus using MPE photochemistry is roughly 10 minutes which is more time than was originally anticipated. To make a larger scale mold with the amount of villi we were originally aiming for to fill a 1 cm by 2 cm sized mold would take around 1-2 days which is far more time than Visar was willing to donate. When the mold goes to fabrication, either a smaller mold will have to be made or a time will have to be found when Visar or someone else who knows how to operate the MPE photochemistry machine has enough time to create the mold.

Testing

On our third meeting with Visar, we visited the Campagnola laboratory in Engineering Centers Building. In the lab, he presented a brief demonstration of the standard operating procedures for creating a polymerized structure using MPE photochemistry. To begin the process, the lights in the lab had to be turned off to prevent any unwanted polymerization. After this, a rubberized circular fence was placed on a microscope slide. This "fence" would serve to pool the polymerizable material, liquid TMPTA, into a volume capable of polymerization. The fence, typically 1 mm in height, allows for the laser to polymerize within its operating range of in the Z-plane. With the fence in place, ~ 40 µL of liquid TMPTA is pipetted in to fill the reservoir. The slide is then transferred onto the microscope; here, the 0 level of the z plane needs to be determined. This calibration is crucial because the fabrication needs to polymerize from the base upwards in order for the solidified TMPTA to adhere to the glass sub-layer and prevent the structure from floating away during fabrication. A fluorescence scan was implemented to find this interface; this results in a sigmoidal curve when the glass-TMPTA interface is found. Once found, Visar imports a stack of image slices and the laser polymerized in the set 800x800 field of view given by the 10x objective used. Parameters he can adjust included power, time/scan, scan rate and area.

Prototype

In order to validate that MPE photochemistry would be able to make a mold with the geometry of conical wells of the dimensions that we needed, we requested that Visar make an initial prototype. He used a sinusoidal curve to make wells with depths of 500µm and diameters of 200µm. After completing the prototype, he he then imaged it with scanning electron microscopy (SEM) so that the wells could be viewed. As seen in Figure 9, the prototype did have conical wells of approximated depth. This demonstrates that we will be able to use this method to make the correct topography of our mold.

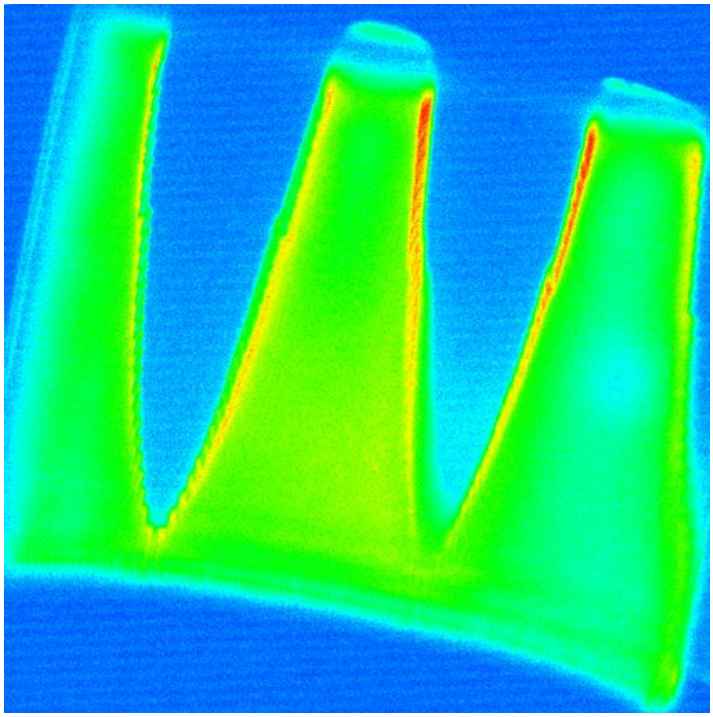

Figure 9: SEM image of initial prototype showing conical shape.

3D Modeling

The next step our project was creating a SolidWorks part of the final mold layout. The first drawing Conor created with SolidWorks was the ideal master mold.

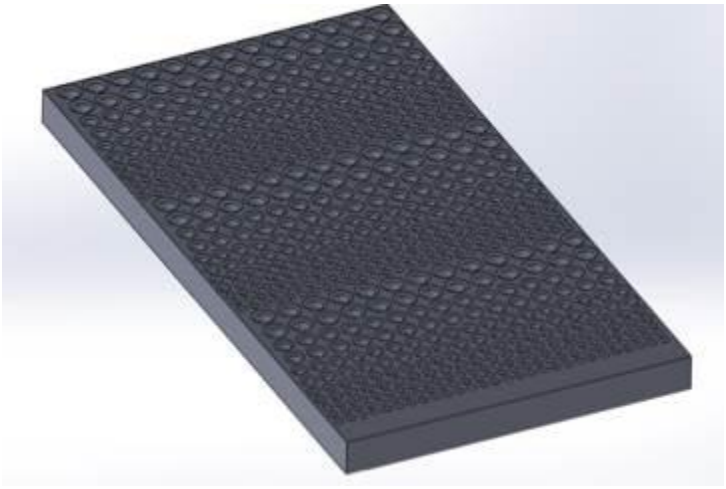

Figure 10: Master mold design in SolidWorks

This mold contains three sections with corresponding heights of 900, 750 or 600 µm. In each of these sections, there are two rows of each diameter starting from 500 microns and ending with 100 µm. The spacing between the bases of each villus is 250 µm. Each of these wells has a tapered conical shape with a few degree tilt from the vertical axis and beveled tips and bases. The total size of the mold is 1 by 2 by 0.1cm.

When we met with Visar, he explained to us that the maximum viewing area of the microscope is 800 by 800 µm. Consequently, this is the largest viewing area in which he can fabricate at one time. Therefore, in order for us to create our entire master mold, we would need to split this up into 800 by 800 micron sections. Instead of creating hundreds of unique pieces, we decided instead to create SolidWorks parts for a single pillar of each diameter and height. We generated 500 micron (which could later be scaled to generate the 400, 300, and 200 micron diameter 2D BMP sequences) and 100 micron diameter villi with heights of 900, 750, and 600 µm. The 100 micron diameter pillars part needs its own SolidWorks file because we were able to fit four pillars in one 800 by 800 micron section while still maintaining the correct spacing.

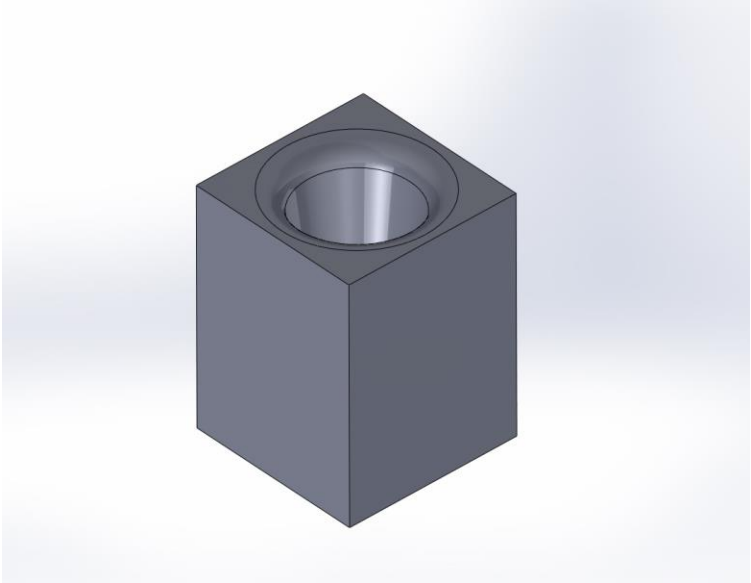

Figure 11: 750x750 µm cross sectional volume taken from master mold featuring a tapered pillar with 500 µm in diameter and 900 µm in depth.

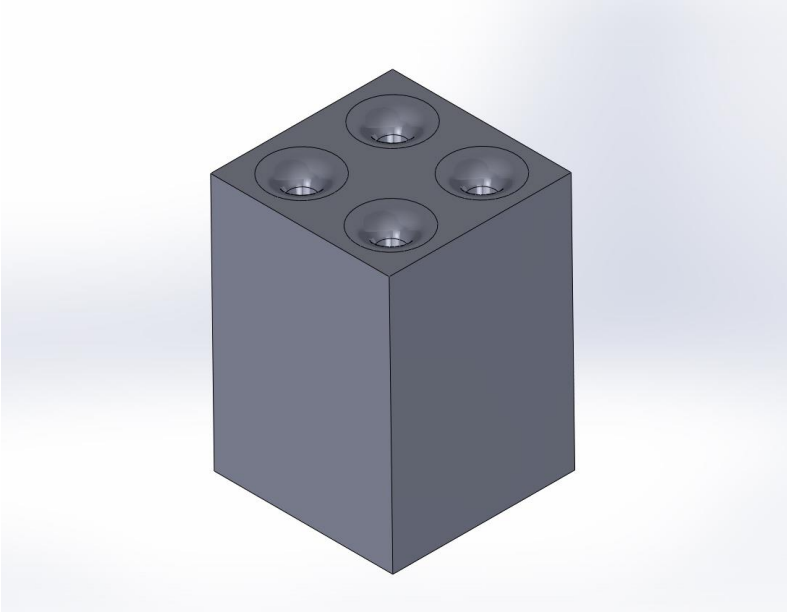

Figure 12: 700x700 µm cross sectional volume taken from master mold featuring four tapered pillars with 100 µm in diameter and 900 µm in depth.

Once we had all six of the SolidWorks parts, the next step was finding a way to slice them into 2D slices. The equipment Visar uses for MPE Photochemistry cannot use a 3D object; instead it needs a sequence of 2D BMP images that it can use to create a 3D model. This is very similar to a 3D printer; however, we have to manually create these 2D images. Therefore, using SolidWorks, we created 333 planes spaced at 3 µm apart and sliced the SolidWorks parts into 333 consequent pieces (Figure 13).

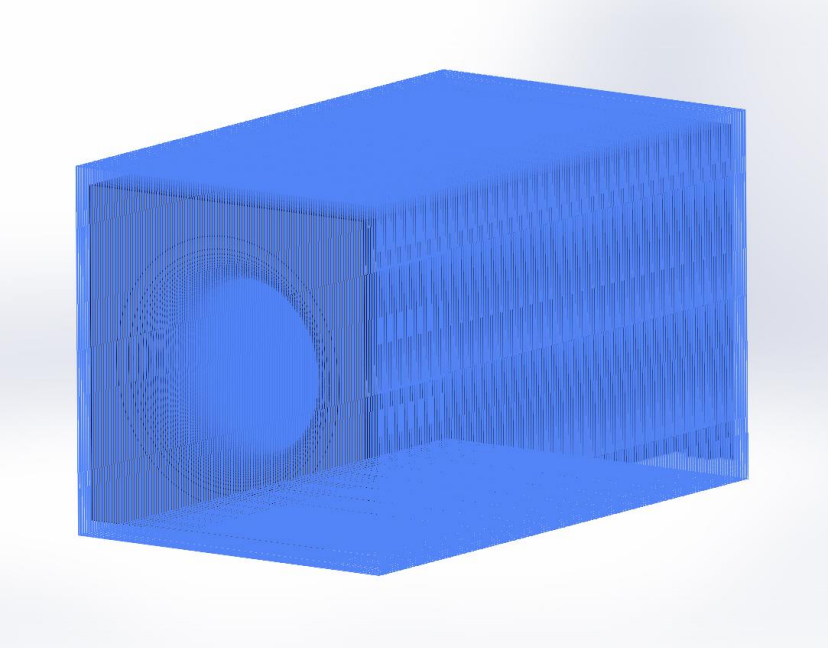

Figure 13: Total volume of 3D pillar structure cut into 333 z-plane cross-sections

SolidWorks saved each of these parts as its own file. Thus, we had to change all of these SolidWorks files into JPEG files. We opened up each SolidWorks slice individually and chose to view them all from the top face to keep consistency. Then, we altered the lighting to "Backdrop – Black with Fill Lights" to change the part to white with black background. Then we saved each as a JPEG.

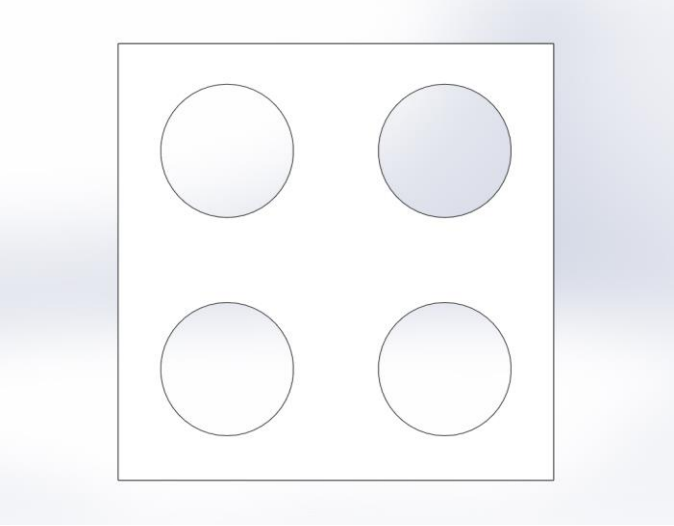

Figure 14: Top view of the 700x700 µm cross section containing pillars of 100 µm diameter

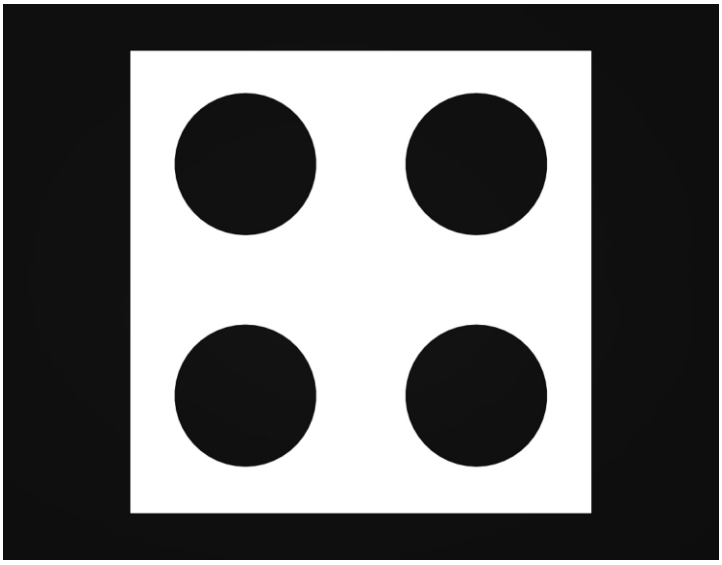

Figure 15: Top view of the 700x700 µm cross section containing pillars of 100 µm diameter converted to an 8-bit, black-and-white JPEG file

Once we had converted all 333 parts into JPEG images similar to the ones seen above, we needed to convert the file type to a BMP. Unfortunately, SolidWorks cannot save as a BMP, therefore we had to use ImageJ to convert from a JPEG to a BMP file type. A BMP file type is different from a JPEG because it is slightly higher resolution and is a much larger file. ImageJ was also able to import all of these files as an image sequence. This put the pictures in the right order for Visar to input so that it would build our 3D cube starting from the base and finishing at the top of the negative mold. We were also able to crop the black background out of the 800 by 800 micron space and scale the image to generate the 400, 300, and 200 micron diameters we wanted. We also needed to invert the colors of the JPEG since black is the part of the image that gets polymerized during MPE Photochemistry. Once we created all 15 BMP sequences with 5 different diameters and 3 different heights, Visar was able to polymerize TMPTA to make a prototype for us.

Final Prototype Analysis

We used bright-field microscopy to image the prototypes Visar created for us in order to determine the accuracy of the MPE method in replicating appropriate mold dimensions. To determine the dimensions of the wells, we imaged our mold along with a grid section of a hemocytometer of known dimension. The hemocytometer grid, which served as a scale, allowed us to find the actual size of our mold features. We took images of the mold using magnifications of 4X, 10X, and 20X. Then, we imported these images into ImageJ, converted the scale to pixels, and applied to the prototype dimensions of the corresponding magnification.

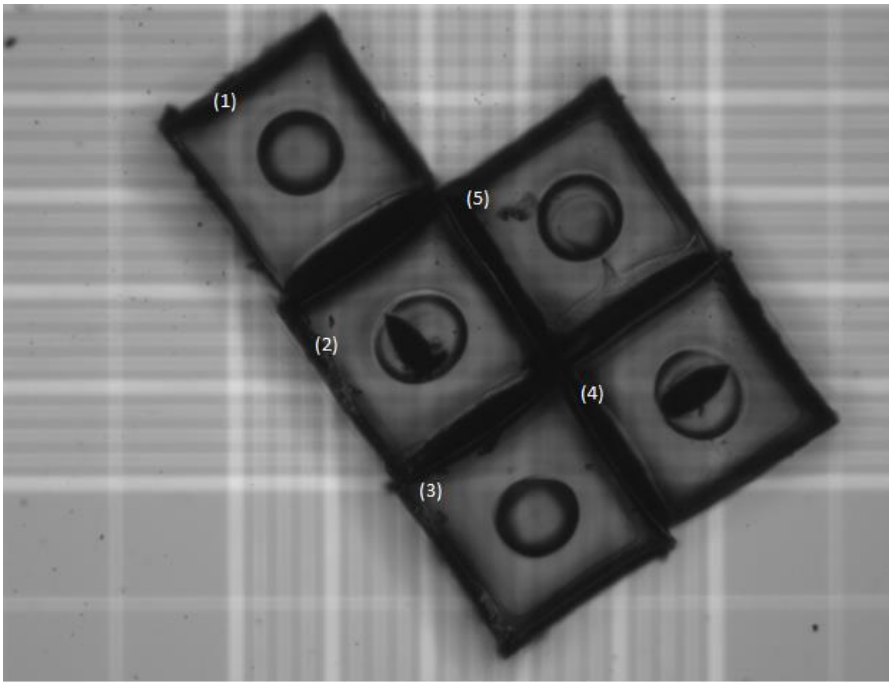

Figure 16: Top down view of final prototypes on hemocytometer grid. Measurements made in Figures 17-18.

Well	Expected Diameter (µm)	Measured Diameter (µm)	Diameter Difference (µm)	Expected Side Length for Spacing (µm)	Measured Side Length (µm)	Side Length Difference (µm)
1	200.000	182.758	-17.242	450.000	416.314	-33.686
2	200.000	202.678	2.678	450.000	423.187	-26.813
3	200.000	189.839	-10.161	450.000	433.382	-16.618
4	200.000	204.592	4.592	450.000	389.082	-60.918
5	200.000	182.312	-17.688	450.000	426.096	-23.904
Average		192.436 ± 9.545			417.612 ± 15.280	

Figure 17: Table describing measurements of prototype pillar diameters, heights, and spacing with standard deviation. Well numbers correspond to numbering of prototypes as shown in Figure 16.

Well	Expected Depth (µm)	Measured Depth (µm)	Depth Difference (µm)
1	900.000	896.435	-3.565
2	750.000	730.528	-19.472
4	600.000	605.056	5.056

Figure 18: Table of measured heights for generated prototypes. No standard deviation depicted due to only having one sample per each height. Well numbers correspond to numbering of prototypes as shown in Figure 16.

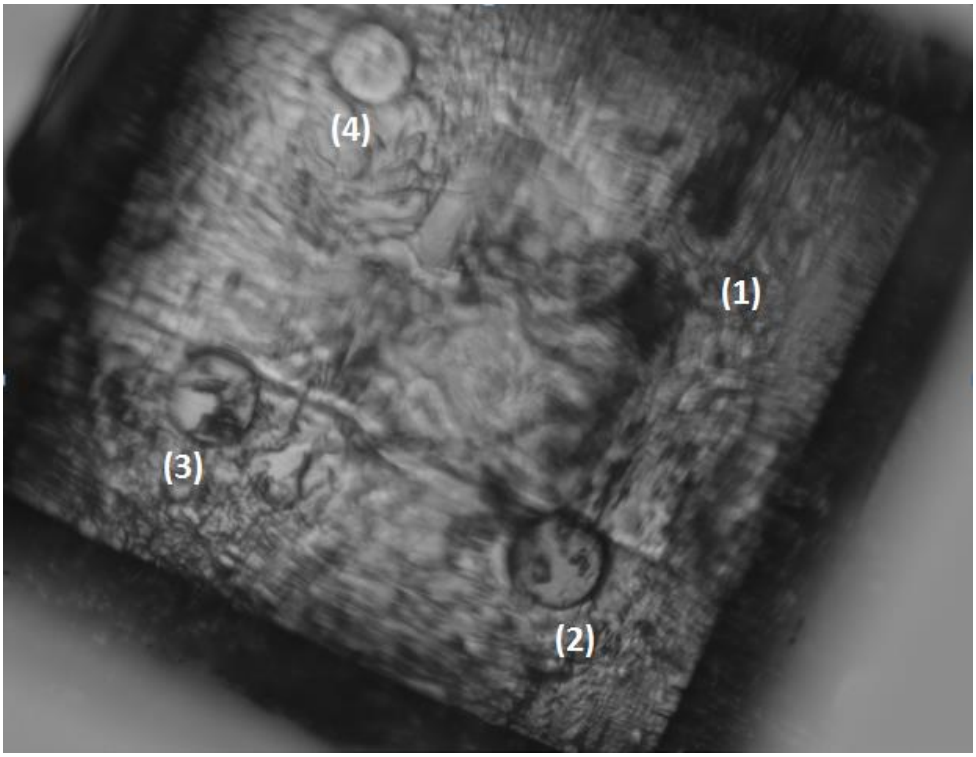

Figure 19: Top down view of 100µm diameter pillar prototypes.

Well	Expected Diameter (µm)	Measured Diameter (µm)	Diameter Difference (µm)
1	100.000	79.124	-20.876
2	100.000	90.500	-9.500
3	100.000	82.297	-17.703
4	100.000	74.781	-25.219
Average		81.676 ± 5.751	

Figure 20: Table of diameters for the 100 µm diameter pillars with actual measurements and standard deviation. Well numbers correspond to numbering of prototypes as shown in Figure 16.

Based on the measurements obtained for our prototypes, we are confident in the ability of MPE photochemistry to fabricate a micro-needle array in the micrometer scale. The discrepancies in the measurements may be due several sources of error, namely, errors in measuring diameter and height due to light refractions on the bright-field microscopy generated images, debris obscuring the diameter and height of the villi in each picture, and damage to the prototypes due to handling. Additionally, we are confident in the ability of MPE photochemistry to fabricate rounded tipped, tapered pillars that resemble the 3D structure of human small intestinal villi.

Future Work

Additional work to be done for the master mold includes rearranging the layout, increasing the range of diameters, heights, and spacing. Furthermore, future work involves

generating the actual master mold. This process would take approximately one to two days to complete. Lastly, following the completion of the master mold, we would need to perform the steps to create the collagen scaffold (Figure 4). As mentioned previously, we may need to add additional steps to the collagen scaffold fabrication process to prevent shear forces from damaging villus architecture integrity.

Acknowledgements

Our team would like to thank Professor Murrell for presenting us the opportunity to assist him in his fascinating research. Through all the hardships and setbacks, Professor Murrell has supported and encouraged us. . It has been a wonderful experience creating the biomimetic intestine for him, and we wish him the best of luck in his future research. We would also like to thank Professor Ashton for his guidance during our project. Without him we never would have made the countless deadlines and noticed the important details. We would like to thank the countless labs we visited when trying to decide on the best method to create this mold. Additionally, we would like to thank Visar Ajeti for his guidance, providing us access to resources and materials in Campagnola lab, and fabricating our prototype and final mold. Finally, a special thanks to the University of Wisconsin-Madison's Department of Biomedical Engineering for their countless resources.

References:

Basson, M.D. 1998. Role of integrins in enterocyte migration. Clinical and Experimental Pharmacology and Physiology 25(3-4):pg 280-285

Bowen, R. (2001, November 1). Villi, Crypts and the Life Cycle of Small Intestinal Enterocytes. *arbl.cvmbs.colostate.edu*. Retrieved October 9, 2013, from http://www.vivo.colostate.edu/hbooks/pathphys/digestion/smallgut/lifecycle.html

Brunicardi, F.C., Andersen, D.K., Billiar, T.R. 2005. Schwartz's Principles of Surgery. 8th edition. McGraw-Hill. New York: NY: p1119-1137

Caceci, T. *Exercise 19: Digestive system 2:intestines*. Retrieved on October 9th, 2013 from http://www.vetmed.vt.edu/education/curriculum/vm8054/Labs/Lab19/Lab19.htm

Chen, X., Su, Y., Ajeti, V., Chen, S.J., Campagnola, P.J., 2012. Cell Adhesion on Micro-Structured Fibronectin Gradients Fabricated by Multiphoton Excited Photochemistry. Cell Mol Bioeng 5(3): p307-319

Gaudet, I.D., Shreiber, D.I. 2012. Characterization of methacrylated type-I collagen as a dynamic photoactive hydrogel. Biointerphases 7(25): p1-9

Gelse, K., Poschl, E., Aigner, T. 2003. Collagens-structure, function, and biosynthesis. Advanced Drug Delivery Reviews 55: p1531-1546

Ghodssi, R., Lin, P., & SpringerLink (Online service). (2010). *MEMS materials and processes handbook*. New York ; London: Springer.

Glowacki, J., Mizuno, S. 2007. Collagen scaffolds for tissue engineering. Biopolymers 89(5): 338-344

Golden, A.P., Tien, J. 2007. Fabrication of microfluidic hydrogels using molded gelatin as a sacrificial element. Lab on a Chip 7(6): p720-725

Jee, H., Sachs, E., A visual simulation technique for 3D printing. 2000. *Advances in Engineering Software*. Retrieved December 10, 2013 from http://www.sciencedirect.com/science /article/pii/S0965997899000459

Lange, B. Microvia forming using UV laser. LPFK Laser & Electronics AG. lpfkusa.com. Retrieved October 8, 2013, from http://www.lpkfusa.com/microline/articles.htm

Lodish, H., Berk, A., Zipursky, S.L. 2000. Collagen: the fibrous proteins of the matrix. Molecular Cell Biology. 4th edition. New York: W.H. Freeman; 2000. Section 22.3. Obtained from http://www.ncbi.nlm.nih.gov/books/NBK21582/

Lorenz, H., Despont, M., Fahrni, N., LaBianca, N., Renaud, P., & Vettiger, P. 1997. SU-8: a low-cost negative resist for MEMS. *Journal of Micromechanics and Microengineering*, *7*(3): p121.

Murrell, M. Assistant Professor. College of Engineering. *University of Madison-Wisconsin*. Retrieved October 9, 2013, from https://directory.engr.wisc.edu/bme/faculty/murrell_michael

Phillips, R., Photopolymerization. 1984. *Journal of Photochemsitry.* Retrieved December 10, 2013 from http://www.sciencedirect.com.ezproxy.library.wisc.edu/science/article/pii/00472 67084850169

Proffitt, T. *Small intestine: Structure and function of the small intestine*. Retrieved on October 9th from http://www.elu.sgul.ac.uk/rehash/guest/scorm/109/package/content

Sachs, E., Cima, M., Cornie, J., Three-Dimensional Printing: Rapid Tooling and Prototypes Directly from a CAD Model. 1990. *CIRO Annals – Manufacturing Technology.* Retrieved December 10, 2013 from http://www.sciencedirect.com/science/article/pii/S000785060761035X

Sherwood, L. 2011. The digestive system. In *Fundamentals of Human Physiology 4th Edition.* Cengage Learning, Stamford, CT. pg 436-476

Sung, J.H., Yu, J., Luo, D., Shuler, M.L., March, J.C. 2011. Microscale 3-D hydrogel scaffold for biomimetic gastrointestinal (GI) tract model. Lab Chip 11: p389-392

Tavakkolizadeh, A., Whang, E.E., Ashley, S.W., Zinner, M.J. Chapter 28 The small intestine. In Schwartz's Principles of Surgery 9th Edition. McGraw Hill Companies Inc. Access online: http://www.accessmedicine.com.ezproxy.library.wisc.edu/resourceTOC.aspx?resourceID=50.

Willerth, S., & Sakiyama-Elbert, S. (n.d.). Combining stem cells and biomaterial scaffolds for constructing tissues and cell delivery | StemBook. *StemBook.* Retrieved October 9, 2013, from http://www.stembook.org/node/450

Waddell, E.A. 2006. Laser ablation as a fabrication technique for microfluidic devices. Methods in Molecular Biology 321: p27-38

Yang, W., Chen, Y., Huang, Y., Fu, Y., Tang, S., Fu, C. 2012. Engineering a biomimetic villus array for in vitro three-dimensional culture of intestinal epithelial cells. Journal of Microelectromechanical systems 21(6): p1418-1425

Yao, D., Smith, A., Nagarajan, P., Vasquez, A., Dang, L., Chaudhry, G.R. Fabrication of polycaprolactone scaffolds using a sacrificial compression-molding process. Journal of Biomedical Materials Research Part B Applied Biomaterials 77B(2): p287-295

Yoo, L. I., Chung, D. C., Yuan, J. 2002. LKB1-A master tumor suppressor of the small intestine and beyond. Nature Reviews Cancer 2: p529-535

Yu, J., Peng, S., Luo, D., March, J.C. 2012. In vitro 3D human small intestinal villous model for drug permeability determination. Biotechnology and Bioengineering 109: p2173-2178

Appendix: Product Design Specifications

Title: Biomimetic Intestine for Traction Force Studies

Team Members: Angela Beltrame, Kevin Knapp, Susanna Kwok, Shaun Pomerenke, Conor Sullivan

Date: September 28, 2013

Problem Statement: The brush border of the human small intestine is comprised of absorptive enterocytes that undergo constant proliferation and bidirectional movement along the villous and crypt folds of the intestine. With a lifespan of twenty-four to forty-eight hours, enterocytes begin their life cycle as stem cells residing in the crypts of the small intestine; as these cells differentiate into mature absorptive enterocytes, they migrate from the crypt to the tip of the villus where they undergo cell death. The intestinal epithelium maintains a dynamic environment in which enterocyte migration from cell production until cell death is held in a stable, coordinated manner. In order study the cellular traction forces responsible for enterocyte migration, an *in vitro* model system mimicking the structure and dimensions of intestinal villi is needed. A biomimetic intestinal environment will be generated using a collagen scaffold mimicking the 3D topography of intestinal villi. Once seeded with epithelial cells, this scaffold will serve as a model to study the cell-cell forces responsible for the movement of epithelial cells in the intestine

Client: Professor Michael Murrell

Design Requirements:

1. Physical and Operational Characteristics
    a. Physical Requirements:
        i. Design must feature methods in generating rounded-tip 3D topographic, micro-needle array mold
        ii. Final mold must be able to generate a 3D collagen hydrogel scaffold
        iii. Cross sectional diameter of villi must be varied
            1. Range of 100µm-500µm
        iv. Height of villus: 600, 750, 900µm
        v. Spacing between villi: 250µm
    b. Safety
        i. Equipment required: UV/CO2 Laser Ablation System
            1. Safety concerns with improper equipment use
        ii. Materials required: TMPTA, methacrylated type-I collagen, phosphate buffer saline (PBS), and fluorescent beads
            1. TMPTA, methacrylated type-I collagen, and fluorescent beads have no safety concerns
    c. Accuracy and Reliability
        i. Mold must generate nearly similar collagen scaffolds having heights of 600, 750 and 900µm and varying in diameter
    d. Life in Service
        i. One semester
    e. Shelf Life

i. Mold used to create 3D collagen scaffold with villi architecture is expected to last several years
ii. Collagen scaffold generated using mold is expected to last several days if not weeks

f. Operating environment
    i. Room temperature (37° C)
    ii. Collagen to be contained in PBS Buffer: pH 7.4
g. Ergonomics
    i. Able to be held in human hand and operable my human hand
    ii. Mold must easily allow scaffold release
h. Size
    i. Scaffold
        1. Villi heights of 600, 750 and 900µm
        2. Villi diameter ranging from 100µm-500µm
    ii. Mold
        1. Millimeter scale: must hold several different micro-needle arrays of varying villi diameters and heights
        2. The mold will hold the following range of villi diameter: 100µm, 200µm, 300µm, 400µm, and 500µm
        3. The mold will hold the following range of villi heights: 600µm, 750µm, 900µm
        4. There will be 250µm spacing between the bases of neighboring villi
        5. The villi will be parabolic conical structures will rounded tips and bases
        6. The final mold will be rectangular with dimensions of 2x1cm and height of 1mm
i. Weight

    TMPTA density = 1.1g/cm^3

        1. Final mold = 1.1g/cm^3(2x1x0.1cm^3) = 0.22g

j. Materials
    i. TMPTA
    ii. Methacrylated type-I collagen
    iii. PBS
    iv. Fluorescent beads
k. Aesthetics, Appearance, and Finish
    i. Rectangular master mold (2x1x0.1cm^3)
    ii. Clear, plastic TMPTA mold.
    iii. Edges to be sanded and smoothed

2. Product Characteristics
    a. Quantity: 1 x Master Mold Prototype
    b. Target Product Cost: <$1000
        i. TMPTA: $45.40 per 100 g
        ii. Methacrylated type-I collagen: $169.50 per 1 liter

iii. PBS: $94.70 per 1 liter
iv. Fluorescent beads: $48.00 per 1 liter

3. Miscellaneous
    a. Standards and Specifications: No international standards or FDA requirements known.
    b. Customer: Professor Murrell would like to be able to create numerous collagen scaffolds based off of our mold. Therefore, he would like a mold that is both reusable and durable. He also would like to be able to view this under a microscope that has a 60x magnification. After our project is completed, Professor Murrell mentioned the possibility of creating his own mold, therefore he would like the process we use to be reproducible. It should be relatively easy and quick for him to follow our method, so we will take this into account when deciding which method to use.
    c. Patent-related concerns: Methodology of mold generation is not patented; therefore we have no patent related concerns.
    d. Competition: A group at Cornell has produced a microarray resembling intestinal villi using a laser-ablation method.